Linear analytical solution to the phase diversity problem for extended objects based on the Born approximation

Raluca M. Andrei*[a], Carlas S. Smith[a], Rufus Fraanje[a], Michel Verhaegen[a], Visa A. Korkiakoski[b], Christoph U. Keller[b] and Niek Doelman[c]

[a]Delft Center for Systems and Control, Mekelweg 2, 2628CD Delft, The Netherlands;
[b]Leiden Observatory, Niels Bohrweg 2, 2333 CA Leiden, The Netherlands;
[c]TNO Science and Industry, Stieltjesweg 1, 2628CK Delft, The Netherlands

ABSTRACT

In this paper we give a new wavefront estimation technique that overcomes the main disadvantages of the phase diversity (PD) algorithms, namely the large computational complexity and the fact that the solutions can get stuck in a local minima. Our approach gives a good starting point for an iterative algorithm based on solving a linear system, but it can also be used as a new wavefront estimation method. The method is based on the Born approximation of the wavefront for small phase aberrations which leads to a quadratic point-spread function (PSF), and it requires two diversity images. First we take the differences between the focal plane image and each of the two diversity images, and then we eliminate the constant object, element-wise, from the two equations. The result is an overdetermined set of linear equations for which we give three solutions using linear least squares (LS), truncated total least squares (TTLS) and bounded data uncertainty (BDU). The last two approaches are suited when considering measurements affected by noise. Simulation results show that the estimation is faster than conventional PD algorithms.

Keywords: point-spread function, wavefront estimation, Born approximation, least squares

1. INTRODUCTION

Phase diversity is a wavefront sensing (WFS) and image reconstruction technique used mostly in post-processing. Due to the fact that this method uses intensity information, it is possibly sensitive to all phase aberrations, as opposed to the conventional Shack-Hartamnn wavefront sensing technique. A serious drawback of the phase diversity method is the long computational time, which is considerable compared to the evolution time of the turbulence. Because of this, efforts have been made to make it faster. Some demonstrations of real-time correction using PD have been obtained for very few corrected aberrations in Refs.[1,2] PD consists of collecting two or more images. One of them is the focal plane image that has been degraded by unknown aberrations. Additional images are obtained by introducing known aberrations into the system. This method was first proposed by Gonsalves[3] for two diversity images and it was based on the minimization of a LS criterion. Since the paper of Gonsalves, the method has been extended and improved in numerous papers.[4–7] Attempts to make PD faster have been made by better numerical algorithms,[8,9] by using object independent error metrics to estimate the aberrations from the data[10] or by different linearization techniques.[11–13]

In this paper we give a new method of real-time wavefront reconstruction using PD. Our approach is based on the Born approximation of the wavefront when the aberrations are small. We give an analytic formula for the PSF which is quadratic in the aberration parameters, using an implicit regularization by the finite series of Zernike polynomials. We subtract from two diversity images (with quadratic PSFs) the focal plane image in order to end up with linear expressions in both the aberration parameters and the object. Further, we eliminate the constant object and end up with an overdetermined linear system in the aberration parameters only. In the noise free case, the system can be solved by linear least squares. A characterization of the diversities which can be used in order for the system matrix to be full column rank is given such that the obtained solution is unique.

Further author information: (Send correspondence to Raluca Andrei)
Raluca Andrei: E-mail: r.m.andrei@tudelft.nl

Adaptive Optics Systems III, edited by Brent L. Ellerbroek, Enrico Marchetti, Jean-Pierre Véran, Proc. of SPIE Vol. 8447, 84476U · © 2012 SPIE · CCC code: 0277-786/12/$18 · doi: 10.1117/12.926119

We also analyse the case where the images are affected by Gaussian white noise and show that we also have to solve a linear system. The difference is that with this system, we have uncertainties both in the A matrix and in the b vector of the linear system $Ax = b$. For this case, we present in Section 4 two additional methods, truncated total least squares[14] (TTLS) and bounded data uncertainty[15] (BDU), which assumes that a-priori bounds on the uncertain data are available.

This paper is structured as follows. Section 2 starts with the quadratic analytical expression of the PSF in terms of the unknown aberration parameters. Section 3 resumes shortly the conventional PD algorithm following Ref.[5] Section 4 is divided into three subsections: in Subsection 4.1 we define the estimation problem formulated as a linear system of equations in the noise free case, in Subsection 4.2 we consider white Gaussian noise and in Subsection 4.3 we give details for the last two solutions to the problem mentioned above, namely TTLS and BDU. Section 5 is dedicated to numerical simulations. Concluding comments are placed in Section 6.

2. ANALYTICAL FORMULA FOR THE PSF

In this section we briefly revise the analytical formulas for the intensity PSF,[16] which will be the starting point of our method. For the derivations we have used the Nijboer-Zernike theory of diffraction integrals containing small aberrations (for more details see Chapter 9 in[17]), which apply to optical systems where the pupil is large compared with the wavelength of the light used. In order to be able to analytically model the PSF we use the Zernike polynomials for the representation of the wavefront.[18] We assume here that the optical system introduces a wavefront aberration only and that the amplitude distribution over the wavefront is uniform. The aberration function Φ is expanded as a Zernike series

$$\Phi(\rho,\theta) = \sum_{n,m} Z_n^m(\rho,\theta)\,\alpha_n^m + Z_n^{-m}(\rho,\theta)\,\alpha_n^{-m} = \sum_{n,m} R_n^m(\rho)\left(\alpha_n^m \cos m\theta + \alpha_n^{-m}\sin m\theta\right), \tag{1}$$

where $Z_n^m(\rho,\theta) = R_n^m(\rho)\cos m\theta, Z_n^{-m}(\rho,\theta) = R_n^m(\rho)\sin m\theta$ are the even and odd Zernike polynomials which form an orthonormal basis on the unit disk, $R_n^m(\rho)$ are called radial polynomials, $n \geq 0$ is the radial degree of the corresponding Zernike polynomial, $m \geq 0$ is the azimuthal frequency, and $n - m \geq 0$ and even.

Under the assumption that Φ is sufficiently small, we can linearize the wavefront

$$\exp(i\Phi(\rho,\theta)) \approx 1 + i\Phi(\rho,\theta). \tag{2}$$

It is easily seen that the Born approximation is a Taylor approximation of the wavefront in 0. We could also use another expansion point resulting in a slightly different linear expression, but we do not go into details here. With Eq. (1) we obtain

$$\exp(i\Phi(\rho,\theta)) \approx 1 + i\sum_{n,m} R_n^m(\rho)\left(\alpha_n^m \cos m\theta + \alpha_n^{-m}\sin m\theta\right). \tag{3}$$

After some derivations, the intesity PSF can be written as

$$j(r,\varphi) = c_0 + \boldsymbol{c_1}^T\boldsymbol{\alpha} + \boldsymbol{\alpha}^T Q\boldsymbol{\alpha}, \tag{4}$$

where $\boldsymbol{\alpha} \in \mathbb{R}^{N_\alpha}$, $\boldsymbol{\alpha} = \begin{bmatrix} \alpha_0^0 & \alpha_1^{-1} & \alpha_1^1 & \alpha_2^0 & \alpha_2^{-2} & \alpha_2^2 & \dots \end{bmatrix}^T$ is the unknown aberration and $c_0 \in \mathbb{R}$, $\boldsymbol{c_1} \in \mathbb{R}^{N_\alpha}$, $Q \in \mathbb{R}^{N_\alpha \times N_\alpha}$[16] are quantities derived from the first principles. These coefficients can also be computed from input and output data through an identification procedure.

Eq. (4) gives a way to compute the intensities in the focal planes as functions of the Zernike coefficients $\boldsymbol{\alpha}$ corresponding to the aberration function Φ. Given a grid of size $M \times N$ and using Eq. (4) for each point of this grid, the intensity PSF can be written as

$$t_0(\boldsymbol{\alpha}) = \begin{bmatrix} j(r_{11},\varphi_{11}) & j(r_{12},\varphi_{12}) & \dots & j(r_{1N},\varphi_{1N}) \\ j(r_{21},\varphi_{21}) & j(r_{22},\varphi_{22}) & \dots & j(r_{2N},\varphi_{2N}) \\ \vdots & \vdots & \vdots & \vdots \\ j(r_{M1},\varphi_{M1}) & j(r_{M2},\varphi_{M2}) & \dots & j(r_{MN},\varphi_{MN}) \end{bmatrix}. \tag{5}$$

The PSF in Eq. (5) can be rewritten as a quadratic function of $\boldsymbol{\alpha}$

$$t_0(\boldsymbol{\alpha}) = C_0 + C_1(I_N \otimes \boldsymbol{\alpha}) + Q_t(I_N \otimes \boldsymbol{\alpha} \otimes \boldsymbol{\alpha}), \tag{6}$$

where $\otimes$ denotes the Kronecker product[19] , I_N is the identity matrix of order N, and the coefficients $C_0 \in \mathbb{R}^{M\times N}$, $C_1 \in \mathbb{R}^{M\times(N_\alpha N)}$, $Q_t \in \mathbb{R}^{M\times\left({N_\alpha}^2 N\right)}$ are given below

$$C_0 := \begin{bmatrix} c_0(r_{11}) & c_0(r_{12}) & \dots & c_0(r_{1N}) \\ c_0(r_{21}) & c_0(r_{22}) & \dots & c_0(r_{2N}) \\ \vdots & \vdots & \ddots & \vdots \\ c_0(r_{M1}) & c_0(r_{M2}) & \cdots & c_0(r_{MN}) \end{bmatrix},$$

$$C_1 := \begin{bmatrix} {\boldsymbol{c_1}}^T(r_{11},\varphi_{11}) & {\boldsymbol{c_1}}^T(r_{12},\varphi_{12}) & \dots & {\boldsymbol{c_1}}^T(r_{1N},\varphi_{1N}) \\ {\boldsymbol{c_1}}^T(r_{21},\varphi_{21}) & {\boldsymbol{c_1}}^T(r_{22},\varphi_{22}) & \dots & {\boldsymbol{c_1}}^T(r_{2N},\varphi_{2N}) \\ \vdots & \vdots & \ddots & \vdots \\ {\boldsymbol{c_1}}^T(r_{M1},\varphi_{M1}) & {\boldsymbol{c_1}}^T(r_{M2},\varphi_{M2}) & \cdots & {\boldsymbol{c_1}}^T(r_{MN},\varphi_{MN}) \end{bmatrix}, \tag{7}$$

$$Q_t := \begin{bmatrix} \tilde{Q}(r_{11},\varphi_{11})^T & \tilde{Q}(r_{12},\varphi_{12})^T & \dots & \tilde{Q}(r_{1N},\varphi_{1N})^T \\ \tilde{Q}(r_{21},\varphi_{21})^T & \tilde{Q}(r_{22},\varphi_{22})^T & \dots & \tilde{Q}(r_{21},\varphi_{21})^T \\ \vdots & \vdots & \ddots & \vdots \\ \tilde{Q}(r_{M1},\varphi_{M1})^T & \tilde{Q}(r_{M1},\varphi_{M1})^T & \dots & \tilde{Q}(r_{MN},\varphi_{MN})^T \end{bmatrix}.$$

Here $\tilde{Q} := \mathrm{vec}(Q)$ is a vector obtained by stacking together all the columns of the matrix Q from left to right. The coefficients in Eq. (7) do not have to be compute in real-time, but are precomputed.

3. PHASE DIVERSITY

Phase diversity consists of recording one focal plane image and one or more additional images using a known diversity (unusually defocus). If d_0 and d_1 are the observed focused and defocused images and t_0 and t_1 are the corresponding PSFs at the moment of exposure, then their relations with the object f are

$$\begin{array}{rcccl} d_0 & = & t_0(\boldsymbol{\alpha}) * f & + & n_0 \\ d_1 & = & t_1(\boldsymbol{\alpha}) * f & + & n_1, \end{array} \tag{8}$$

where $*$ denotes convolution, t_0 is given by Eq. (6), t_1 is given by

$$t_1(\boldsymbol{\alpha}) = t_0(\boldsymbol{\alpha} + \boldsymbol{\alpha}_{d1}), \tag{9}$$

$\boldsymbol{\alpha}_{d1}$ is a known quantity and n_0, n_1 represent measurement noise. The minimized error metric in the PD algorithm (see for example Refs.[3–5]) measures the sum of the square errors in the difference between the observed images and the ones obtained from the reconstructions

$$L = \sum_{u,v} |D_0 - \hat{F}\hat{T}_0|^2 + |D_1 - \hat{F}\hat{T}_1|^2, \tag{10}$$

where $\hat{}$ denotes an estimate value, u and v spatial frequencies and F, D_0, D_1, T_0, T_1 are the Fourier transforms of f, d_0, d_1, t_0, t_1. The optimum restored object, F_M, is found by minimizing L considering known aberrations

$$F_M = \left(|\hat{T}_0|^2 + |\hat{T}_1|^2\right)^{-1}\left(D_0\hat{T}_0^* + D_1\hat{T}_1^*\right) \tag{11}$$

Substituting the object from Eq. (11) in Eq. (10) we obtain the modified error metric

$$L_M = \sum_{u,v} \left(|\hat{T}_0|^2 + |\hat{T}_1|^2\right)^{-1}\left(D_1\hat{T}_0 - D_0\hat{T}_1\right). \tag{12}$$

4. LINEAR PROBLEM

In this section we formulate our estimation problem as a linear system of equations and give the three solutions mentioned in the introduction. We start the presentation with the noise free case and then we incorporate the noise following the same steps.

4.1 The noise free case

For this part, we assume we have obtained three images, one focus plane image d_0, and diversity images d_1 and d_2, with PSFs t_0 in Eq. (6) and $t_k,\ k = 1 \dots 2$, such that

$$t_k(\boldsymbol{\alpha}) = t_0(\boldsymbol{\alpha} + \boldsymbol{\alpha}_{dk}),\ k = 1, 2, \tag{13}$$

where $\boldsymbol{\alpha}_{dk}$ are known quantities. As stated in the previous section, the images are obtained as a convolution of the PSF with the object f

$$\begin{aligned} d_0 &= t_0(\boldsymbol{\alpha}) * f \\ d_k &= t_k(\boldsymbol{\alpha}) * f,\ k = 1, 2. \end{aligned} \tag{14}$$

The approach we use here is to subtract from each diversity image the focus plane image

$$d_{dk} = d_k - d_0 = [t_k(\boldsymbol{\alpha}) - t_0(\boldsymbol{\alpha})] * f = [t_0(\boldsymbol{\alpha} + \boldsymbol{\alpha}_{dk}) - t_0(\boldsymbol{\alpha})] * f,\ k = 1, 2. \tag{15}$$

We use further Eq. (6) to write down expressions for the two PSFs in Eq. (15) and obtain

$$\begin{aligned} d_{dk} &= [C_1(I_N \otimes \boldsymbol{\alpha}_{dk}) + Q_t(I_N \otimes \boldsymbol{\alpha}_{dk} \otimes \boldsymbol{\alpha}_{dk} + I_N \otimes \boldsymbol{\alpha} \otimes \boldsymbol{\alpha}_{dk} + I_N \otimes \boldsymbol{\alpha}_{dk} \otimes \boldsymbol{\alpha})] * f \\ &= \left[C_1(I_N \otimes \boldsymbol{\alpha}_{dk}) + Q_t(I_N \otimes \boldsymbol{\alpha}_{dk} \otimes \boldsymbol{\alpha}_{dk}) + 2\sum_{i=1}^{N_\alpha} \alpha_i v_{ki}\right] * f,\ k = 1, 2, \end{aligned} \tag{16}$$

where

$$v_{ki} = Q_t(I_N \otimes e_i \otimes \boldsymbol{\alpha}_{dk}),\ i = 1 \dots N_\alpha \tag{17}$$

and $e_i = \begin{bmatrix} \dots & 0 & 1_i & 0 & \dots \end{bmatrix}^T$. With

$$p_k := C_1(I_N \otimes \boldsymbol{\alpha}_{dk}) + Q_t(I_N \otimes \boldsymbol{\alpha}_{dk} \otimes \boldsymbol{\alpha}_{dk}),\ k = 1, 2, \tag{18}$$

we get

$$d_{dk} = \left(p_k + 2\sum_{i=1}^{N_\alpha} \alpha_i v_{ki}\right) * f,\ k = 1, 2. \tag{19}$$

We take the Fourier transform in Eq. (19) and using the notations $D_{dk} := \mathcal{F}\{d_{dk}\},\ P_k := \mathcal{F}\{p_k\},\ V_{ki} := \mathcal{F}\{v_{ki}\}, F := \mathcal{F}\{f\}$ (of dimension $M_\mathcal{F} \times N_\mathcal{F}$), we get

$$D_{dk} = \left(P_k + 2\sum_{i=1}^{N_\alpha} \alpha_i V_{ki}\right) \odot F,\ k = 1, 2, \tag{20}$$

where $\odot$ denotes point-wise multiplication.

Next we show that the unknown aberration parameters can be determined by solving a linear system. To this end, we can write

$$\begin{aligned} D_{d1} &= \left(P_1 + 2\sum_{i=1}^{N_\alpha} \alpha_i V_{1i}\right) \odot F, \\ D_{d2} &= \left(P_2 + 2\sum_{i=1}^{N_\alpha} \alpha_i V_{2i}\right) \odot F. \end{aligned} \tag{21}$$

Because the object is the same we can divide the two equations element by element and cross multiply the terms to obtain

$$D_{d1} \odot \left(P_2 + 2\sum_{i=1}^{N_\alpha} \alpha_i V_{2i} \right) = D_{d2} \odot \left(P_1 + 2\sum_{i=1}^{N_\alpha} \alpha_i V_{1i} \right), \tag{22}$$

or

$$D_{d1} \odot P_2 - D_{d2} \odot P_1 = 2\sum_{i=1}^{N_\alpha} \alpha_i \left(D_{d2} \odot V_{1i} - D_{d1} \odot V_{2i} \right). \tag{23}$$

Using the notation $\tilde{X} = \mathrm{vec}\,(X)$ for the vectorized variants of the terms of Eq. (23), we can write it as

$$A\boldsymbol{\alpha} = b, \tag{24}$$

where $A \in \mathbb{C}^{M_\mathcal{F} N_\mathcal{F} \times N_\alpha}$, $b \in \mathbb{C}^{M_\mathcal{F} N_\mathcal{F}}$ and

$$\begin{aligned} b &= \tilde{D}_{d1} \odot \tilde{P}_2 - \tilde{D}_{d2} \odot \tilde{P}_1, \\ A &= \left[\tilde{D}_{d2} \odot \tilde{V}_{11} \;\; \tilde{D}_{d2} \odot \tilde{V}_{12} \;\; \ldots \;\; \tilde{D}_{d2} \odot \tilde{V}_{1N_\alpha} \right] - \left[\tilde{D}_{d1} \odot \tilde{V}_{21} \;\; \tilde{D}_{d1} \odot \tilde{V}_{22} \;\; \ldots \;\; \tilde{D}_{d1} \odot \tilde{V}_{2N_\alpha} \right]. \end{aligned}$$

The least squares solution to Eq. (24) is $\boldsymbol{\alpha} = (A^* A)^{-1} A^* b$.

We have to make a remark with respect to the two diversities used in the algorithm. If $\boldsymbol{\alpha}_{d1}$ and $\boldsymbol{\alpha}_{d2}$ both correspond to diversities of Zernike modes with odd radial degree n (we will call this an odd diversity) or with even radial degree n (we will call this an even diversity), respectively, then $\ker(A) \neq \emptyset$ and the solution of Eq. (24) is not unique.

We can prove this statement by considering two odd diversities $\boldsymbol{\alpha}_{d1}$ and $\boldsymbol{\alpha}_{d2}$. The matrices $v_{1i},\ i = 1 : N_\alpha$ and $v_{2i},\ i = 1 : N_\alpha$ in Eq. (17) will have only zero elements for even i. This translates, after vectorization, in zero even columns of the A matrix. Because A has a non-empty kernel, only the unknowns corresponding to odd n can be computed uniquely. The same type of reasoning holds true for two even diversities.

4.2 The white Gaussian noise case

Let us consider that the measuremets d_0, d_1, d_2 are affected by Gaussian white noise.

$$\begin{aligned} d_0 &= t_0(\boldsymbol{\alpha}) * f + n_0 \\ d_k &= t_k(\boldsymbol{\alpha}) * f + n_k,\ k = 1, 2. \end{aligned} \tag{25}$$

The corresponding Eqs. (21) will then be

$$\begin{aligned} D_{d1} &= \left(P_1 + 2\sum_{i=1}^{N_\alpha} \alpha_i V_{1i} \right) \odot F + N_{10}, \\ D_{d2} &= \left(P_2 + 2\sum_{i=1}^{N_\alpha} \alpha_i V_{2i} \right) \odot F + N_{20}, \end{aligned} \tag{26}$$

where $N_{k0} = \mathcal{F}\{n_k - n_0\},\ k = 1, 2$. Assuming that the quantities in the brackets in Eq. (26) are not zero we obtain

$$\begin{aligned} D_{d1} \oslash \left(P_1 + 2\sum_{i=1}^{N_\alpha} \alpha_i V_{1i} \right) &= F + N_{10} \oslash \left(P_1 + 2\sum_{i=1}^{N_\alpha} \alpha_i V_{1i} \right), \\ D_{d2} \oslash \left(P_2 + 2\sum_{i=1}^{N_\alpha} \alpha_i V_{2i} \right) &= F + N_{20} \oslash \left(P_2 + 2\sum_{i=1}^{N_\alpha} \alpha_i V_{2i} \right), \end{aligned} \tag{27}$$

where $\oslash$ denotes point-wise divison. Eliminating the object, we end up with

$$D_{d2} \oslash \left(P_2 + 2\sum_{i=1}^{N_\alpha} \alpha_i V_{2i} \right) - D_{d1} \oslash \left(P_1 + 2\sum_{i=1}^{N_\alpha} \alpha_i V_{1i} \right) = N_{20} \oslash \left(P_2 + 2\sum_{i=1}^{N_\alpha} \alpha_i V_{2i} \right) - N_{10} \oslash \left(P_1 + 2\sum_{i=1}^{N_\alpha} \alpha_i V_{1i} \right), \tag{28}$$

or

$$D_{d2}\odot\left(P_1+2\sum_{i=1}^{N_\alpha}\alpha_i V_{1i}\right)-D_{d1}\odot\left(P_2+2\sum_{i=1}^{N_\alpha}\alpha_i V_{2i}\right)=N_{20}\odot\left(P_1+2\sum_{i=1}^{N_\alpha}\alpha_i V_{1i}\right)-N_{10}\odot\left(P_2+2\sum_{i=1}^{N_\alpha}\alpha_i V_{2i}\right). \quad (29)$$

With

$$\begin{aligned}\delta b &= \tilde{N}_{10}\odot\tilde{P}_2-\tilde{N}_{20}\odot\tilde{P}_1\\ \delta A &= \left[\begin{array}{cccc}\tilde{N}_{20}\odot\tilde{V}_{11} & \tilde{N}_{20}\odot\tilde{V}_{12} & \ldots & \tilde{N}_{20}\odot\tilde{V}_{1N_\alpha}\end{array}\right]-\left[\begin{array}{cccc}\tilde{N}_{10}\odot\tilde{V}_{21} & \tilde{N}_{10}\odot\tilde{V}_{22} & \ldots & \tilde{N}_{10}\odot\tilde{V}_{2N_\alpha}\end{array}\right].\end{aligned}$$

we obtain

$$(A+\delta A)\,\boldsymbol{\alpha}=b+\delta b. \quad (30)$$

4.3 Solving the linear system

Both the coefficient matrix and the right-hand side of the overdetermined system of linear equations in Eq. (30) are subject to errors. Additionally to the LS solution, we propose here two other methods to compute the solution of this system, TTLS[14] and BDU[15] , respectively.

Total least squares (TLS)[20] is a method of fitting which was developed to deal with linear models $Ax\approx b$ with both sides affected by errors, exactly as in the case of Eq. (30). In the TLS method one allows a residual matrix as well as a residual vector, and the computational problem becomes

$$\min_{\delta A,\delta b}\left\|\left[\begin{array}{cc}\delta A & \delta b\end{array}\right]\right\|_F \quad \text{subject to } (A+\delta A)\,x=b+\delta b. \quad (31)$$

The TLS technique has been traditionally applied to problems that are numerically rank deficient. The idea is to simply treat the small singular values of $\left[\begin{array}{cc}A & b\end{array}\right]$ as zeros. This technique is called truncated TLS (TTLS). The almost redundant information in $\left[\begin{array}{cc}A & b\end{array}\right]$, associated with the small singular values, is discarded and the original ill-conditioned problem is replaced with another nearby and more well-conditioned problem. The TTLS algorithm, given in[14] , can be summarized as follows:

Algorithm TTLS

1. Compute the SVD of the augmented matrix $\left[\begin{array}{cc}A & b\end{array}\right]$:

$$\left[\begin{array}{cc}A & b\end{array}\right]=U\Sigma V^*=\sum_{i=1}^{N_\alpha+1}u_i\sigma_i v_i^*,\ \sigma_1\geq\ldots\geq\sigma_{N_\alpha+1}. \quad (32)$$

2. Choose a truncation parameter $k\leq\min\left(N_\alpha,\operatorname{rank}\left[\begin{array}{cc}A & b\end{array}\right]\right)$ such that

$$\sigma_k>\sigma_{k+1}\text{ and }V_{22}\equiv\left[\begin{array}{ccc}v_{N_\alpha+1,k+1} & \ldots & v_{N_\alpha+1,N_\alpha+1}\end{array}\right]\neq 0. \quad (33)$$

3. Partition the matrix V such that (with $q=N_\alpha-k+1$)

$$V = \begin{array}{c}\left[\begin{array}{cc}V_{11} & V_{12}\\ V_{21} & V_{22}\end{array}\right]\begin{array}{c}\}\\ \}\end{array}\begin{array}{c}N_\alpha\\ 1.\end{array}\\ \underbrace{}_{k}\ \underbrace{}_{q}\end{array} \quad (34)$$

4. Compute the minimum-norm TLS solution x_k as

$$x_k=-V_{12}V_{22}^\dagger=-V_{12}V_{22}^*\|V_{22}\|_2^{-2}. \quad (35)$$

In step 2 of the algorithm, the regularization parameter k has to be choosen. A possible stopping criterion can be based on the L-curve[21] . The idea in this method is to plot in a log-log scale the solution norm, $\|x_k\|_2$ versus the residual norm, $\| \left[\begin{array}{cc} A & b \end{array} \right] - \left[\begin{array}{cc} A_k & b_k \end{array} \right] \|_F$, and choose as the optimal k the truncation parameter at which this curve has an L-shaped corner. Essentially, the corner is defined by locating the point with greatest curvature in the log-log scale. For the implementation functions from the Regularization Tools software package[22] can be used.

The second solution that we analyse is a method of parameter estimation in the presence of bounded data uncertainties. In Eq. (30) we assume we can determine an upper bound on the 2-induced norm of the perturbation δA and on the Euclidean norm of δb

$$\|\delta A\|_2 \leq \eta, \quad \|\delta b\|_2 \leq \eta_b. \tag{36}$$

Then, we solve the following problem

$$\min_{\hat{x}} \max\{\| \left(A + \delta A\right) \hat{x} - \left(b + \delta b\right) \|_2 : \|\delta A\|_2 \leq \eta, \|\delta b\|_2 \leq \eta_b\}. \tag{37}$$

The BDU algorithm can be resumed as follows (following Section 3.4 in[15]):

Algorithm BDU

1. Compute the SVD of A

$$A = U \left[\begin{array}{c} \Sigma \\ 0 \end{array} \right] V^* = \left[\begin{array}{cc} U_1 & U_2 \end{array} \right] \left[\begin{array}{c} \Sigma \\ 0 \end{array} \right] V^* = U_1 \Sigma V^*, \; \sigma_1 \geq \ldots \geq \sigma_{N_\alpha}. \tag{38}$$

2. Partition the vector $U^* b$ into

$$\left[\begin{array}{c} b_1 \\ b_2 \end{array} \right] = U^* b. \tag{39}$$

3. Introduce the secular function

$$f\left(\alpha\right) = b_1^* \left(\Sigma^2 - \eta^2 I\right) \left(\Sigma^2 + \beta I\right)^{-2} b_1 - \frac{\eta^2}{\beta^2} \|b_2\|_2^2. \tag{40}$$

4. Define

$$\tau_1 = \frac{\|\Sigma^{-1} b_1\|_2}{\|\Sigma^{-2} b_1\|_2} \text{ and } \tau_2 = \frac{\|A^* b\|_2}{\|b\|_2} \tag{41}$$

5-I. If b does not belong to the column span of A

   a) If $\eta \geq \tau_2$ then the unique solution is $\hat{x} = 0$.

   b) If $\eta < \tau_2$ then the unique solution is $\hat{x} = \left(AA^* + \hat{\beta} I\right)^{-1} A^* b$, where $\hat{\beta}$ is the unique positive root of the secular equation $f\left(\beta\right) = 0$.

5-II. If b belongs to the column span of A

   a) If $\eta \geq \tau_2$ then the unique solution is $\hat{x} = 0$.

   b) If $\tau_1 < \eta < \tau_2$ then the unique solution is $\hat{x} = \left(AA^* + \hat{\beta} I\right)^{-1} A^* b$, where $\hat{\beta}$ is the unique positive root of the secular equation $f\left(\beta\right) = 0$.

   c) If $\eta < \tau_1$ then the unique solution is $\hat{x} = V \Sigma^{-1} b_1 = A^\dagger b$.

   d) If $\eta = \tau_1 = \tau_2$ then there are infinitely many solutions that are given by $\hat{x} = \beta V \Sigma^{-1} b_1 = \beta A^\dagger b$, for any $0 \leq \beta \leq 1$.

The solution of the secular equation is feasible using the above formula, when the entire SVD of the matrix A can be computed. For large, sparse matrices, $\hat{\beta}$ can be computed recursively as it is shown in[23] . We choose a random initial value β_0 and perform the following recursion until the change in variables reaches a given tolerance

$$\beta_k = \eta \frac{\|A\left(A^*A + \beta_k I\right)^{-1} A^* b - b\|_2}{\|\left(A^*A + \beta_k I\right)^{-1}\|_2}. \tag{42}$$

For the computation of η we assume a normal distribution for the SNR in an interval (lb, ub). Accordingly, η is computed in the probabilistic sense using the Randomized Algorithm (RA)[24] . In general, the condition $\eta < \tau_2$ can be assured by the choice of the values of the diversities.

5. SIMULATIONS

We have assumed that the atmospheric turbulence distorts only the phase of the wavefront. We further assume that the statistics of the turbulence are described by the Kolmogorov turbulence model with the outer scale of the turbulence $L_0 = 42$ m, the Fried parameter $r_0 = 0.5$ m. The wavefronts have rms values of 0.3 rad and are written as the series from Eq. (1) with 14 Zernike coefficients. The simulations presented here consider isoplanatic image formation, namely the PSF is considered space invariant on the entire field of view. Due to the fact that in our simulations, TTLS and BDU have not shown improvements with respect to the LS, we only present simulations in the no noise case and give the LS solution.

As stated in Section 2, the coefficients in Eq. (7) of the PSF in Eq. (6) are precomputed using a grid of 128×128 points over a pupil of diameter $D = 1$ m. The pupil is sampled on a 64×64 grid and the observed scene is a standard image from the Image Processing Toolbox of Matlab of 128 pixels.

We have simulated 50 wavefronts with rms values of 0.3 rad. The diversities used are $\alpha_{d1}(6,1)$, $\alpha_{d2}(8,1)$ (where the order of the Zernike coefficients is given in the definition of $\boldsymbol{\alpha}$ in (4)), with values which give a diversity shape of 0.3 rad rms. To show the gain in computational time of our algorithm, we compare the results of PD stopped after 10 iterations or a residual tolerance in the cost function and the estimated coefficients of $1e-3$ with the LS solution. In Fig. 1 we plot the mean and variance of the absolute values of the differences between estimated and real parameter values for each Zernike coefficient (on the left) and the computational times and the ratios of computational times between PD and LS, respectively for the 50 runs of the simulation (on the right).

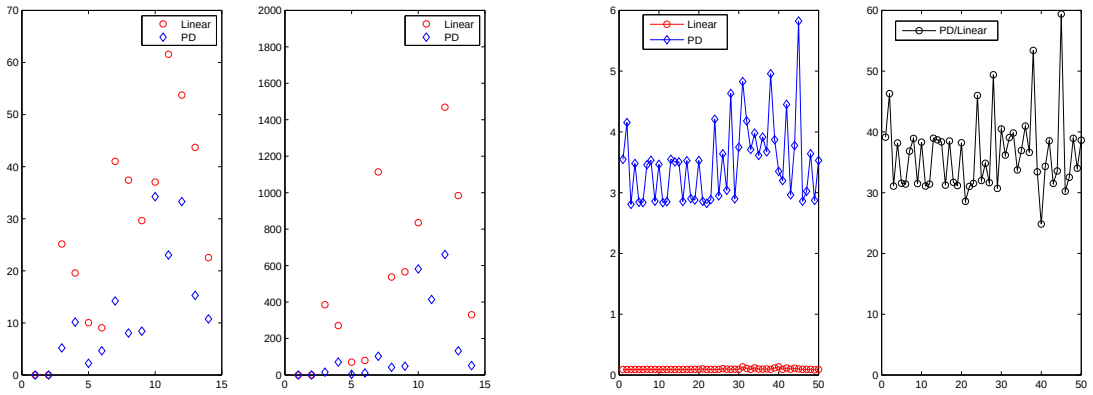

(a) Mean and variance of the absolute values of the differences between estimated and real parameter values (in radians);

(b) Computational times;

Figure 1: Simulation of PD and the linear algorithm with 50 experiments

We also validate the possible usage of our approach as a starting point for PD in Fig. 2. To this end we give two plots, showing the aberration parameters obtained by initializing the PD with zero, the other obtained by initializing PD with the LS solution, and the real Zernike coefficients. The PD algorithm was stopped when the residual error reached a tolerance of $1e-3$.

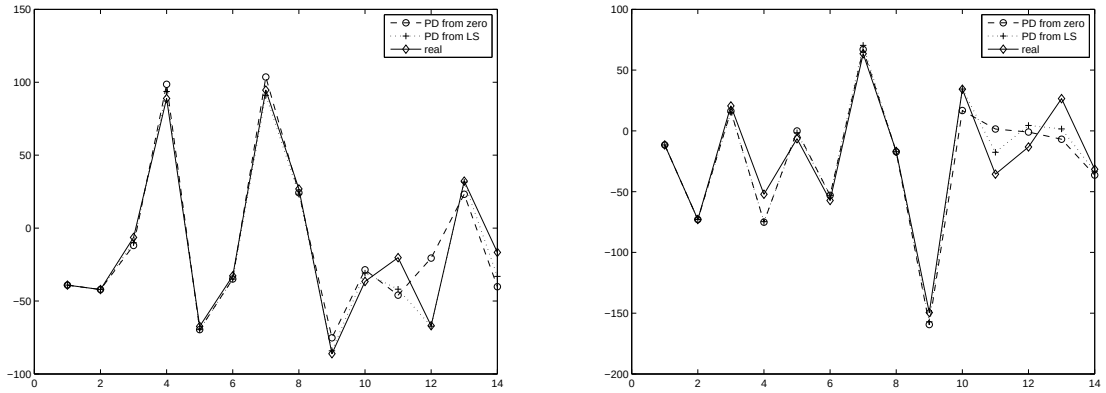

(a) Real and estimated Zernike coefficients (in radians) (I);

(b) Real and estimated Zernike coefficients (in radians) (II);

Figure 2: Simulation of PD with different initial points

6. CONCLUSIONS

We have developed a new method for phase aberration estimation in case of imaging through turbulence using phase diversity. This method is based on the linearization of the wavefront for small values of the aberrations. Using two diversity images we are able to reformulate the problem as an overdetermined system of linear equations. In the noise-free case, this system is solved with the linear least squares algorithm and in the presence of Gaussian white noise three solution methods were presented. Results show that this approach is faster than the PD algorithm. This proves that our method has real potential to be used in a real-time adaptive optics system.

REFERENCES

[1] E.L. Gates, S.R. Restaino, R.A. Carreras, R.C. Dymale, and G.C. Loos, "Phase diversity as an on-line wavefront sensor: experimental results," *Proc. SPIE* **2302**, 330–339 (July 1994).

[2] R.L. Kendrick, D.S. Acton, and A.L. Duncan, "Experimental results from the lockheed phase diversity test facility," *Proc. SPIE* **2302**, 312–322 (July 1994).

[3] Gonsalves, R. A., "Phase retrieval and diversity in adaptive optics," *Optical Engineering* **21**, 829–832 (1982).

[4] R. G. Paxman, T. J. S. and Fienup, J. R., "Joint estimation of object and aberrations by using phase diversity," *Journal of Optical Society of America A* **9**, 1072–1085 (1992).

[5] Lofdahl, M. and Scharmer, G. B., "Wavefront sensing and image restoration from focused and defocused solar images," *Astronomy & Astrophysics Supplement Series* **107**, 243–264 (1994).

[6] Thelen, B., Paxman, R., Carrara, D., and Seldin, J., "Maximum a *posteriori* estimation of fixed aberrations, dynamic aberrations, and the object from phase-diverse speckle data," *Journal of Optical Society of America A* **16**(5), 1016–1025 (1999).

[7] Blanc, A., Mugnier, L., and Idier, J., "Marginal estimation of aberrations and image restoration by phase diversity," *Journal of Optical Society of America A* **20**(6), 1035–1045 (2003).

[8] C.R. Vogel, Chan, T., and Plemmons, R., "Fast algorithms for phasediversity-based blind deconvolution," *Adaptive Optical System Technologies* **3353**, 994–1005 (1998).

[9] Lofdahl, M., Duncan, A., and Scharmer, G., "Fast phase diversity wavefront sensor for mirror control," *Adaptive Optical System Technologies* **3353**, 952–963 (1998).

[10] Scharmer, G., "Object-independent fast phase-diversity," *High Resolution Solar Physics: Theory, Observations and Techniques* **183**, 330–341 (1999).

[11] Gonsalves, R., "Small-phase solution to the phase-retrieval problem," *Optics letters* **26**(10), 684–685 (2001).

[12] Wild, W. J., "Linear phase retrieval for wave-front sensing," *Optics letters* **23**(8), 573–575 (1998).

[13] Mocœur, I., Mugnier, L., and Cassaing, F., "Analytical solution to the phase-diversity problem for real-time wavefront sensing," *Optics letters* **34**(22), 3487–3489 (2009).

[14] Fierro, R. D., Golub, G. H., Hansen, P. C., and O'leary, D. P., "Regularization by truncated total least squares," *SIAM J. Sci. Comput.* **18**(4), 1223–1241 (1997).

[15] Chandrasekaran, S., Golub, G. H., Gu, M., and Sayed, A. H., "Parameter estimation in the presence of bounded data uncertainties," *SIAM. J. Matrix Anal. & Appl.* **19**(1), 235–252 (1998).

[16] Andrei, R., Smith, C., Fraanje, R., Verhaegen, M., Korkiakoski, V. A., Keller, C. U., and Doelman, N., "Bilinear solution to the phase diversity problem for extended objects based on the born approximation," (2012). submitted to SPIE Astronomical Telescopes and Instrumentation.

[17] Born, M. and Wolf, E., [*Principles of Optics*], Pergamon, Oxford, UK (1985).

[18] Noll, R., "Zernike polynomials and atmospheric turbulence," *Journal of Optical Society of America* **66**(3), 207–211 (1976).

[19] Brewer, J. W., "Kronecker products and matrix calculus in system theory," *IEEE Transactions on Circuits and Systems* **CAS-25**, 772–781 (1978).

[20] Markovsky, I. and Huffel, S. V., "Overview of total least squares methods," *Signal Processing* **87**, 2283–2302 (2007).

[21] Hansen, P. C. and O'Leary, D. P., "The use of the l-curve in the regularization of discrete ill-posed problems," *SIAM J. Sci. Comput.* **14**, 1487–1503 (1993).

[22] Hansen, P. C., "Regularization tools: A matlab package for analysis and solution of discrete ill-posed problems," *Numerical Algorithms* **6**, 1–35 (1994).

[23] Haber, A., Fraanje, P., and Verhaegen, M., "Fast and robust iterative learning control for lifted systems," *Proceedings of the 18th IFAC World Congress* **18** (August 2011).

[24] Calafiore, G., Dabbene, F., and Tempo, R., "A survey of randomized algorithms for control synthesis and performance verification," *Journal of Complexity* **23**(3), 301–316 (2007).